2017 IEEE-RAS 17th International Conference on
Humanoid Robotics (Humanoids)
Birmingham, UK, November 15-17, 2017

Biped Walking Pattern Generation based on Spatially Quantized Dynamics

Shuuji Kajita[1], Mehdi Benallegue[1], Rafael Cisneros[1], Takeshi Sakaguchi[1], Shin'ichiro Nakaoka[1]
Mitsuharu Morisawa[1], Kenji Kaneko[1], Fumio Kanehiro[1]

***Abstract*— We present a biped walking pattern generation based on a new way of system discretization named spatially quantized dynamics (SQD). In SQD, a continuous system is discretized by a constant unit length along the walk direction, and the dynamics is represented by a recurrence formula for a unit length motion, taking variable period for each cycle. Using SQD modelling, we can generate a biped gait by taking three steps; 1) Design a walking pattern only considering kinematics in the sagittal plane, 2) Calculate the ZMP and velocity by optimization of the spatially quantized dynamics, 3) Add hip lateral motion for 3D dynamic balance. It is shown that we can easily generate a biped gait with stretched knees and a gait for large step climbing. The validity of the generated patterns are confirmed by simulations.**

I. INTRODUCTION

One of the practical methods for biped gait generation and control is originated by Vukobratović and Stepanenko[1]. Their idea was to design the center of pressure of the target robot first, then to calculate its joint angles by using inverse dynamics with consideration of convergence of the trajectory. They called the center of pressure Zero-Moment Point (ZMP) since the horizontal components of the floor reaction moment become zero at the point, thus the method is usually referred as ZMP based gait generation.

The ZMP based method was firstly applied to a real biped robot by Takanishi et al.[2]. Also, the Honda's humanoid robots use ZMP for their walk control [3].

During the last fifteen years, the ZMP concept has yielded fruitful results. For example, we can see the preview control based pattern generator [4], the analytical solution using piecewise polynomials of ZMP [5], the method by model predictive control and quadratic programming [6], the method by differential dynamic programming [7], and the method using closed-form solution of LQR problem [8].

In this paper, we propose yet another ZMP based gait generation by using a novel way of system modelling, named Spatially Quantized Dynamics (SQD). It helps us to generate a gait of long stride by exploiting fully stretched knees as shown in Fig.1.

In this paper, we explain our method in step-by-step manner. Section II explains the generation of spatial walking pattern, in which we design sagittal walking motion as a function of horizontal position of the hip. It is important that

[1]The authors are with Intelligent Systems Institute, AIST, 1-1-1 Umezono, Tsukuba, Ibaraki 305-8560, Japan {s.kajita, mehdi.benallegue, rafael.cisneros, sakaguchi.t, s.nakaoka, m.morisawa, k.kaneko, f-kanehiro}@aist.go.jp

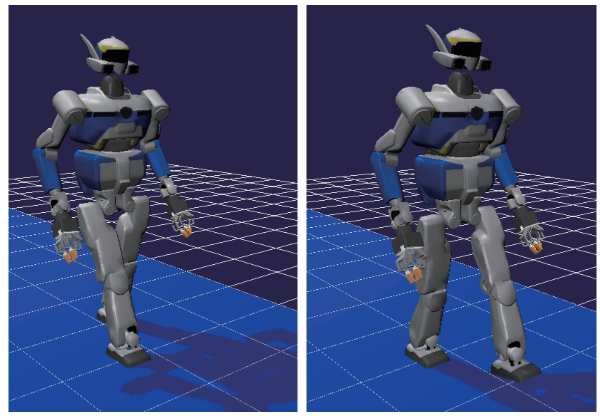

Fig. 1. HRP-2Kai walk simulation using Spatially Quantized Dynamics (1s,50cm per step)

we do not concern any static/dynamic balance at this step. In section III, we introduce the spatially quantized dynamics (SQD) of a linear inverted pendulum, and shows dynamic gait generation by optimization. The optimization is applied in space domain and the result can be transformed into time domain by simple calculation. In section IV, a lateral motion generation for 3D balance is presented and it is blended with the sagittal pattern obtained in the preceding sections. The gait is validated by a dynamic simulation in section V. We also present a gait generation of step climbing and its simulation. In section VI and VII, we compare our method with other methods having some similarities. Section VIII concludes this paper and our future plan is expressed.

II. SPATIAL WALKING PATTERN

In the first process of our walking pattern generation, we design a kinematic gait in the sagittal plane.

For the target robot, we use the model of humanoid robot HRP-2Kai which has 1.71m height, 65kg weight [9]. Its total degrees of freedom (DoF) are 32, however, we only treat its leg part which has 12 DoF.

Figure 2 shows a sagittal gait pattern in which HRP-2Kai takes three 0.5m steps. In this walking, the horizontal hip position x changes from 0m to 1.5m, and we discretize it with a resolution of 1mm. First, we designate the hip position at the moment of each heel landing and each toe lifting. At these moments, the robot must fully extend both of the knees as shown by dark color. For the rest of x positions, the legs are specified to have the fully extended support knee and to lift the foot at a desired height from the floor (drawn with thin color).

From above conditions, we can uniquely determine the hip height and the pitch joint angles for all moments of walking. To robustly solve these inverse kinematics under singularities, we used Levenberg-Marquardt method modified by Sugihara [10]. Note that, we account neither static nor dynamic balance of walking at this stage.

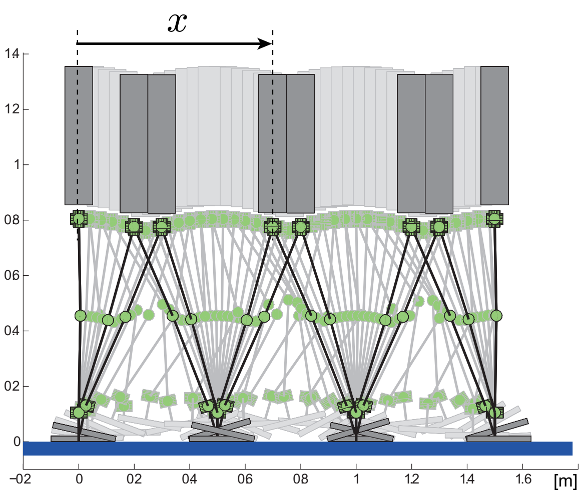

Fig. 2. Spatial waling pattern

Figure 3 shows the joint angle profiles corresponding to the walking pattern of Fig.2. The graphs show the hip pitch, knee pitch, and ankle pitch angles of right and left legs for the sagittal walking motion. It is important that the patterns are defined as functions of horizontal hip position x (see Fig.2) and are not functions of time.

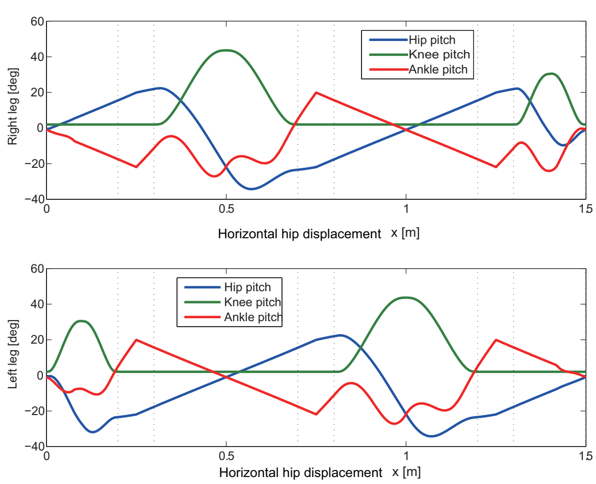

Fig. 3. Spatially defined joint angles

III. Spatially quantized dynamics

In this section, we transform the spatial walking pattern into time domain in consideration of dynamic balance specified by Zero-Moment Point.

A. Target ZMP and target speed

To keep dynamic balance during walking and to realize desired walking speed, we specify the reference ZMP and reference speed as functions of the horizontal hip position (Fig.4). In the upper graph, the shaded area indicates the support polygon determined by the walking pattern, and the reference ZMP is designed to be inside of the area. The reference velocity is specified to reach the target speed 0.5m/s at the first step and to stop at the last step.

As it was already explained, the references are specified as the function of the horizontal waist position. Therefore, we have not specified any information for the timing of the gait. The walking pattern in time domain is obtained by the optimization process in the following subsections.

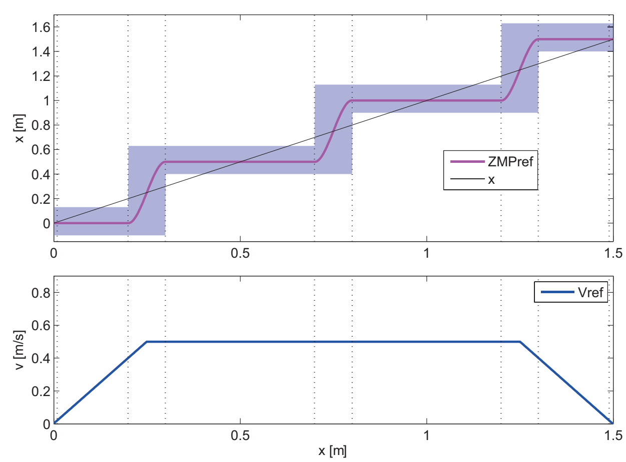

Fig. 4. Target ZMP and target speed

B. LIPM and spatially quantized dynamics

Figure 5 shows the relationship between the waist position and the center of mass (CoM) under the spatial walking pattern.

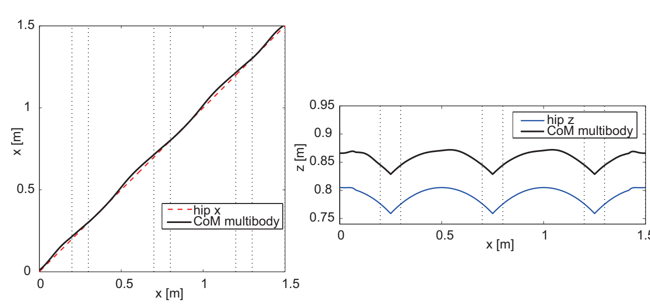

Fig. 5. Relationship between the waist position and the center of mass

Since the CoM position has a good correspondence with the horizontal hip displacement, we can expect that the robot dynamics can be expressed by the linear inverted pendulum model (LIPM)[11], [12]. The equation of motion is given by following

$$\ddot{x} = \omega^2(x - p) \tag{1}$$
$$\omega := \sqrt{g/z},$$

where x is the hip horizontal displacement, p is the ZMP, and g is gravity acceleration. The CoM height z is specified as the average CoM height of the spatial gait.

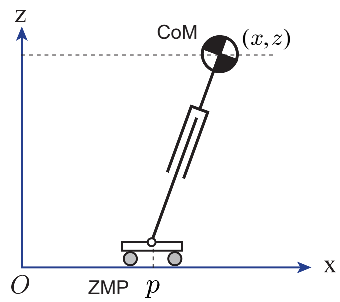

Fig. 6. Cart-pendulum model

Now, we spatially discretize this dynamics by using a constant unit length Δx. That means, we determine the i-th CoM position as follows, taking i as an index for discretization.

$$x_i = \Delta x \cdot i \quad (i = 0, 1, 2, \ldots) \tag{2}$$

In this paper, we used $\Delta x = 0.001$m for spatial discretization.

If we had the CoM speed v_i as known, the time for which CoM travels from x_i to x_{i+1} is given as

$$\Delta t_i = \frac{\Delta x}{v_i}. \tag{3}$$

Using this variable time step Δt_i which depends on speed and the acceleration of LIPM (1), we can calculate the CoM speed at the next spatial step.

$$v_{i+1} = v_i + \omega^2(x_i - p_i)\frac{\Delta x}{v_i} \tag{4}$$

We call this the Spatially Quantized Dynamics (SQD) of LIPM. Note that we have the velocity in the denominator of the second term in the right hand side. This makes our equation nonlinear and we cannot apply linear control theory. In addition, it is necessary

$$\|v_i\| > \epsilon, \tag{5}$$

where ϵ is the lowest speed to avoid divide-by-zero. In this paper we used $\epsilon = 0.005$m/s.

C. From temporal to spatial quantization

The above introduced method drastically changes the view of discretization of continuous systems. Here, we would like to review its implication.

Conventionally, we have naturally assumed that time is a uniformly quantized parameter as

$$t_i = \Delta t \cdot i \quad (i = 0, 1, 2, \ldots), \tag{6}$$

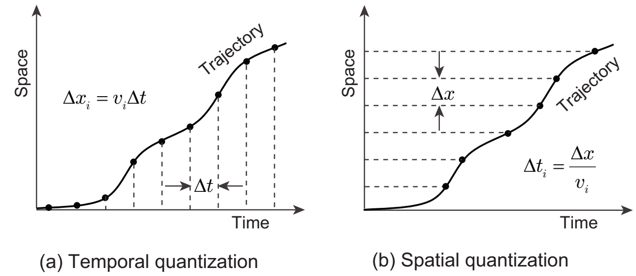

Fig. 7. Two methods of discretization

where Δt is a constant time step. The state variable is updated in every time step, for example, with Δt =5ms. For a general mechanical system, the velocity is updated as

$$v_{i+1} = v_i + \frac{dv_i}{dt}\Delta t. \tag{7}$$

where dv_i/dt is the acceleration of the system.

The updated velocity determines the spatial displacement for each cycle.

$$\Delta x_i = v_i \Delta t \tag{8}$$

This traditional framework is shown in Fig.7(a), and let us call it a *temporal quantization* of a continuous dynamic system.

Now, we can conceive its complementary concept, a *spatial quantization* which is illustrated as Fig. 7(b). In this framework, a position variable is uniformly quantized as

$$x_i = \Delta x \cdot i \quad (i = 0, 1, 2, \ldots),$$

where Δx is a constant spatial step (ex. Δx =1mm). Then the velocity of a system is updated as

$$v_{i+1} = v_i + \frac{dv_i}{dt} \cdot \frac{\Delta x}{v_i}. \tag{9}$$

It is important to notice that an increment of index i does not correspond to the unit time, but to the unit spatial displacement. In this paper, we call a system obtained by a spatial quantization Spatially Quantized Dynamics (SQD).

We can understand SQD as a metaphor of a roller coaster. That is, a trajectory of SQD is spatially fixed like a track of a roller coaster, while we can still control its running speed. This change of viewpoints from temporal to spatial quantization brings us an unprecedented simplification of biped walking pattern generation, as described below.

D. Optimization and space-time conversion

What we need is to calculate a walking pattern which tracks the references (III-A) while satisfying the spatially quantized dynamics (III-B). This can be formalized as the following optimization problem.

$$\begin{aligned} \underset{p_i}{\text{minimize}} \quad & J := \sum_{i=1}^{N}(v_i - v_i^{ref})^2 + \beta(p_i - p_i^{ref})^2 \\ \text{subject to} \quad & v_{i+1} = v_i + \omega^2(x_i - p_i)\frac{\Delta x}{v_i}, \\ & \|v_i\| > \epsilon, \end{aligned} \tag{10}$$

where N is the size of the reference trajectory and β is a scalar weight to control the trade-off between ZMP and speed tracking accuracy.

To solve this optimization problem, we used the Matlab toolbox of Differential Dynamic Programming (DDP) developed by Tassa, Mansard, and Todorov [13]. Figure 8 shows the optimization result using different weights $\beta = 1, 50$. The upper graph shows the ZMP trajectories with its reference (broken line) and the support polygon (shaded area). The ZMP obtained by $\beta = 1$ is shown by thin magenta line, which does not track the reference well. Since the ZMP eventually leaves the support polygon (at 0.3s and 0.8s), it may induce unstable contact between the support sole and the floor. On the other hand, the ZMP obtained by $\beta = 50$ (bold red line) shows accurate track to the reference. This ZMP is well kept inside of the support polygon, and we can expect a stable dynamic walk.

The lower graph of Fig.8 shows the obtained CoM speed profiles and its reference (broken line). The velocity profile obtained by $\beta = 1$ is shown by the thin blue line, which approximately tracks the reference. The velocity obtained by $\beta = 50$ (bold green line) shows undulation apart from the reference. In terms of robot actuation, this walking pattern requires higher joint speed than the former one.

Considering the above mentioned trade-off, we decided to use $\beta = 50$ for stable dynamic gaits with accurate control of ZMP.

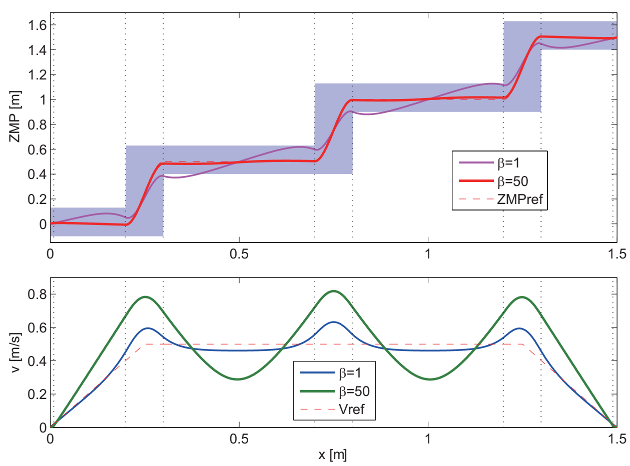

Fig. 8. ZMP and velocity by DDP optimization

To convert the spatial pattern into time domain, we calculate the time for the i-th spatial reference data by using following equation.

$$t_i = \sum_{n=1}^{i-1} \frac{\Delta x}{v_n} \tag{11}$$

Figure 9 shows the time profile of the ZMP and the velocity obtained in Fig.8 ($\beta = 50$). In this graph, we can observe that the single support periods are about 1.3s for walk start and end, while they are 1s during steady walking (from 3s to 5.3s). Those step timing and double support periods are automatically determined as the result of optimization. Likewise, we can obtain the joint angle profile in time domain from the spatial pattern of Fig.3 and the time (11).

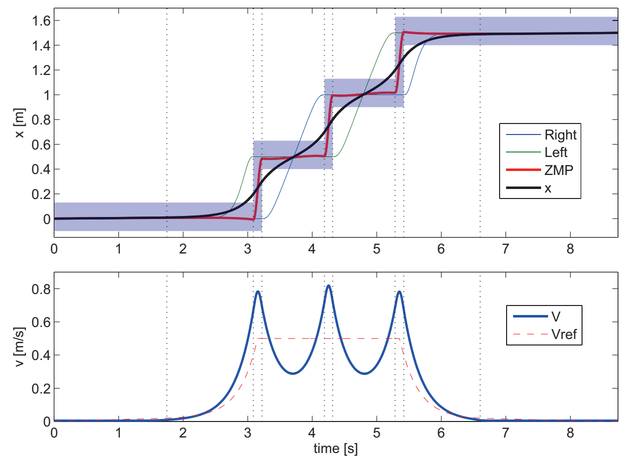

Fig. 9. Gait pattern in time domain ($\beta = 50$)

IV. Lateral Motion Generation

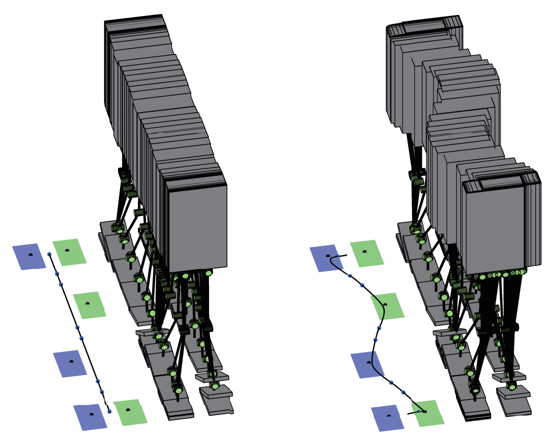

Fig. 10. Adding lateral motion for 3D dynamic gait

So far, we have only discussed walking pattern generation in the sagittal plane and no lateral balance was considered (Fig.10 left). To establish 3D dynamic walking, we must add lateral sway motion as illustrated in Fig.10 right.

We designed a lateral hip motion based on the timing obtained in the previous section and LIPM dynamics using Capture point (also known as Divergent Component of Motion and extrapolated center of mass)[14], [15], [16].

In our method, the reference capture point is kept in the support foot and moved to reach the new support foot at the moment of next touchdown. The lateral hip motion can be calculated from this reference capture point by a simple calculation. The joint trajectories for 3D walk are obtained by adding the desired hip lateral motion to the sagittal

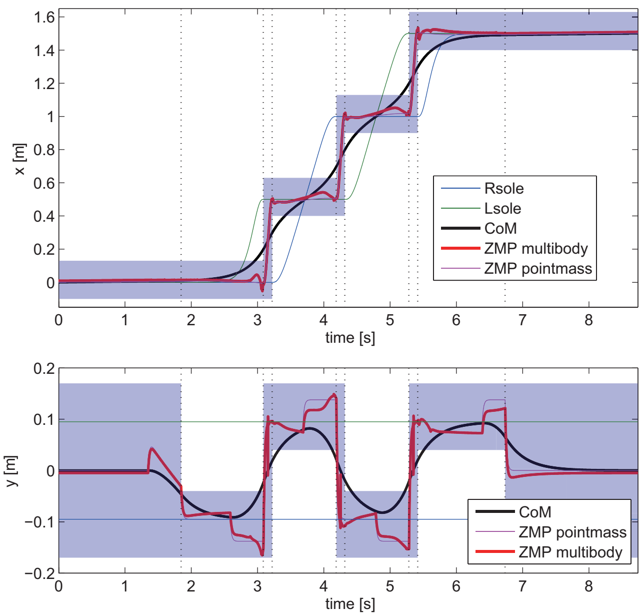

Fig. 11. ZMP calculated by multibody model using obtained gait

walking pattern while keeping the original feet positions and orientations.

Figure 11 shows the ZMP calculated from the multibody dynamics of HRP-2Kai humanoid robot under the obtained 3D walking pattern. Although we designed the walking pattern using simple point mass model, the ZMP is kept inside of support polygon in the entire walking sequence.

V. SIMULATIONS

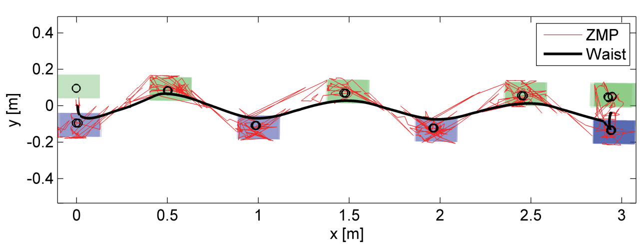

Fig. 12. Simulation of six step walking

We simulated biped walk on the Choreonoid which is an integrated GUI software developed by Nakaoka [17]. First we applied playback control with offline generated walking pattern and found the unstable behavior due to the landing impact at each touchdown. To solve this problem, we used a stabilizer based on the trunk position compliance control proposed by Nagasaka et al.[18]. The simulated robot could realize walk of 50cm step with stretched support knees as shown in Fig.1.

A walk simulation result for longer distance is shown in Fig.12. The plotted ZMP, waist motion, and foot prints illustrate a successful walking gait under the walking pattern of six 50cm steps. Due to the small slip of each step, the resulting path was shifted about 5cm to the right from the planned route and was 5% shorter. Nevertheless, we could realize a reliable knee stretched walk with big stride.

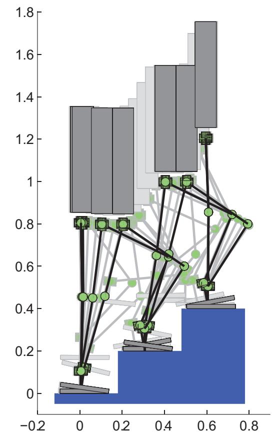

Fig. 13. Spatial walking patterns for climbing steps

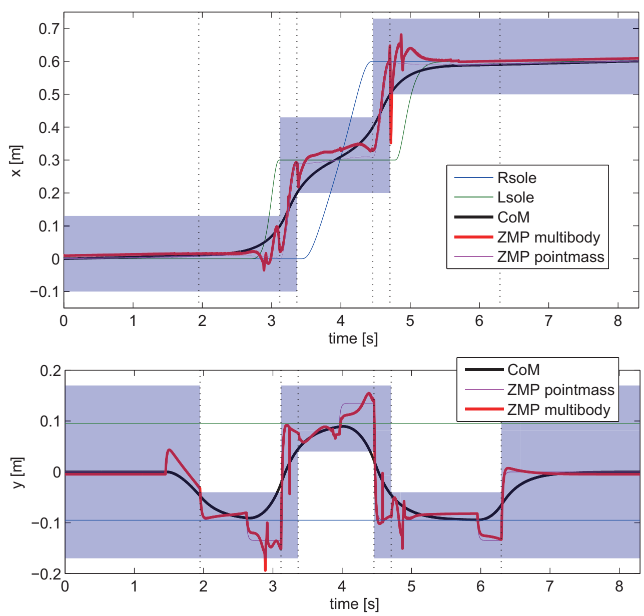

Fig. 14. ZMP for the climbing pattern

As another example, we designed a walking pattern to go up two 20cm height steps. Figure 13 shows the spatial pattern, where the robots at the instants of walk start, foot touchdown, foot liftoff, and walk end are drawn in dark color. In this walking pattern, we designed the hip height trajectory so that the knee joint fully extends at the end of each support phase. By this way, the robot can maximally exploit its mechanical property.

To obtain the sagittal climbing motion, we designed appropriate reference ZMP and horizontal speed as we specified in III-A. Then we calculated the ZMP and the horizontal speed by the optimization of III-D. Note that we can still use the LIPM dynamics to approximate a robot whose CoM height

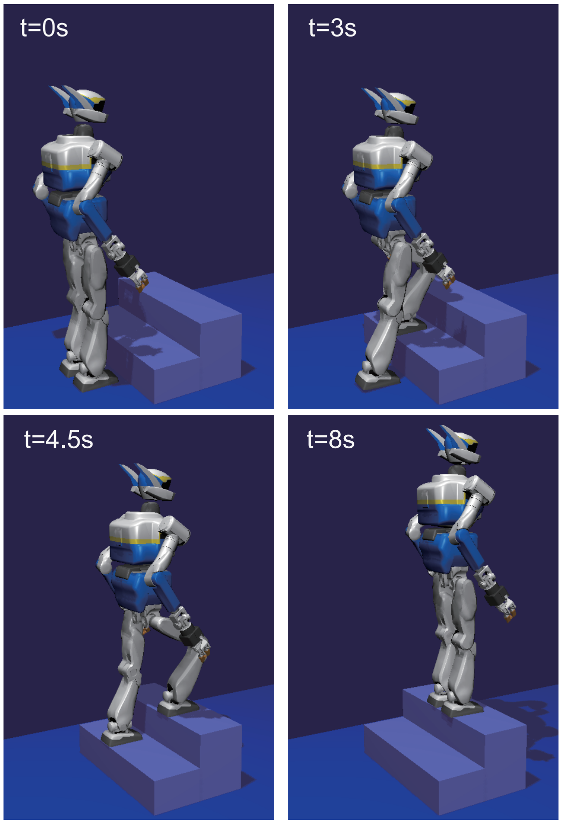

Fig. 15. Simulation of climbing two 20cm steps

varies in time.

$$\ddot{x} = \omega^2(x - p)$$
$$\omega := \sqrt{g/z},$$

This is guaranteed by the nature of the linear inverted pendulum model (LIPM) [11] but the reference CoM height z should be calculated by the following average

$$z := \frac{1}{N}\sum_{i=1}^{N} z_i^{ref} - p_{z,i}^{ref}, \tag{12}$$

where z_i^{ref} is the height of the CoM of the spatial walking pattern, and $p_{z,i}^{ref}$ is the height of the ZMP reference.

By optimizing the sagittal motion, we could determine the step timing, then the lateral sway motion was calculated and merged as explained in Section IV. To check the validity of the generated 3D motion, we calculated the ZMP using multibody model of HRP-2Kai and it is shown in Fig. 14. The multibody ZMP (bold red lines) shows irregularities caused by the large leg motion for the climbing. Nevertheless, they mostly stay inside the support polygons (shaded area) except the spikes at 4.7s in the x-direction and at 2.9s in y-direction. These spikes were caused by discontinuities of the planned trajectory, and we can expect it does not harm the entire balance of walking. Indeed a stable climbing was realized in the simulation by using this walking pattern as shown in Fig.15.

In our method, collision avoidance between the legs and the environment is solved in spatial pattern generation and walking patterns of different speed can be generated after that. Therefore, it can simplify a walking control in cluttered environment compared with the conventional methods.

VI. Comparison with the Hybrid Zero Dynamics based Control

In this section, we compare our method with the zero dynamics based walking control which has some similar concepts.

The zero dynamics is originated in nonlinear control theory to handle complicated dynamic systems. In 2003, Westervelt, Grizzle, and Koditschek proposed a control based on zero dynamics of planer biped walkers [19]. They called their robot dynamics Hybrid Zero Dynamics (HZD), because it is a hybrid system which consists impact dynamics of support leg exchanges.

The hybrid zero dynamics is also used in the recent biped robot research, for example, there have been developed AMBER2, a 2D biped robot which can perform a human-like gait with heel-strike and double support [20] and DURUS, a 3D biped humanoid robot designed for efficient locomotion [21], [22].

Let us look at the case of AMBER2 biped robot [20]. In this control, the most important state variable is the linearized forward position δp_{hip} of the hip measured from the support foot as shown in Fig.16. Having a target hip velocity as

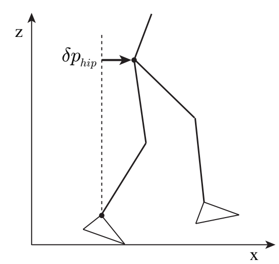

Fig. 16. Parameter definition of Partial Hybrid Zero Dynamics walk control[20]

constant ν_{hip}, the desired hip position is at time t is defined as

$$\delta p_{hip}^d = \nu_{hip} t. \tag{13}$$

From this definition, the local time for each step is parametrized as following.

$$\tau = (\delta p_{hip} - \delta p_{hip}^+)/\nu_{hip}, \tag{14}$$

where δp_{hip}^+ is the hip position at the beginning of current step. The target joint angles for each step cycle are calculated as the function the local time τ.

The differences between SQD and PHZD (a version of HZD) can be summarized as following. Both methods uses optimization to generate walking patterns, whereas the SQD trajectory is optimized in spatial domain and PHZD trajectory is optimized in time domain. For the system dynamics, SQD uses a template model (LIPM) while PHZD uses full dynamics of the robot. In SQD, we define the robot configuration as a function of hip position in global coordinate (x in Fig.2) while PHZD uses local hip position (δp_{hip} in Fig.16).

VII. Time-scaling and SQD

Our method can be regarded as a time-scaling to satisfy dynamic constraint. Traditionally, a time-scaling is implemented by introducing a scalar path coordinate $s(t)$ and a state variable $x(s)$ as its function. Then the velocity is given by

$$v(t) := \frac{d}{dt}x(s(t)) = \frac{dx}{ds} \cdot \frac{ds}{dt}. \tag{15}$$

Therefore, the term (ds/dt) provides an extra degree of freedom to control the system. Such parameterization was used for trajectory optimization by Verscheure et al.[23] and Hauser [24]. Their works and our method are sharing the common concept; a decoupling of kinematic planning and dynamic feasibility.

On the other hand, our spatially quantized dynamics enable a time-scaling without use of extra variables in discrete domain.

$$v_i = \frac{\Delta x}{t_{i+1} - t_i}. \tag{16}$$

It is important to notice the index i is associated with the spatial displacement whose increment of Δx corresponds to $i+1$. By this assignment, we can treat t_i as an independent variable which represents a time-scaling.

VIII. CONCLUSIONS

The essential idea of Vukobratović and Stepanenko was to generate a biped gait from a pre-defined time profile of reference ZMP[1]. While their idea was greatly contributed to realize reliable biped robot walking, it has introduced difficulty in fully exploiting the mechanical possibility. That is, the gait generation based on the prescribed ZMP time function tend to force conservative gait design, and as its symbolic effects, “crouch walking of robots” were widely observed in the biped robot community.

The walking pattern generation based on spatially quantized dynamics can unleash the biped robots from the harness of ZMP as time function, and can realize versatile gait generation with fully deployment of robot's mechanical property. Currently, we are expanding our method for walk direction change, uneven terrains, and external force adaptations toward human level agility of biped locomotion.

References

[1] M.Vukobratović and J.Stepanenko, “On the Stability of Anthropomorphic Systems,” *Mathematical Biosciences*, vol. 15, pp. 1–37, 1972.

[2] A.Takanishi, Hun-ok Lim, M.Tsuda, and I.Kato, “Realization of dynamic biped walking stabilized by trunk motion on a sagittally uneven surface,” in *Proceedings of IEEE International Workshop on Intelligent Robots and Systems*, 1990, pp. 323–330.

[3] K.Hirai, M.Hirose, Y.Haikawa, and T.Takenaka, “The development of honda humanoid robot,” in *Proceedings of the 1998 IEEE International Conference on Robotics & Automation*, 1998, pp. 1321–1326.

[4] S.Kajita, F.Kanehiro, K.Fujiwara, K.Harada, K.Yokoi, and H.Hirukawa, “Biped Walking Pattern Generation by using Preview Control of Zero-Moment Point,” in *Proceedings of IEEE International Conference on Robotics and Automation(ICRA)*, 2003.

[5] K.Harada, S.Kajita, K.Kaneko, and H.Hirukawa, “An analytical method for real-time gait planning for humanoid robots,” *International Journal of Humanoid Robotics*, vol. 3, no. 1, pp. 1–19, 2006.

[6] P.-B. Wieber, “Trajectory free linear model predictive control for stable walking in the presence of strong perturbations,” in *Proceedings of IEEE-RAS International Conference on Humanoid Robots*, 2006, pp. 137–142.

[7] S.Feng, X.Xinjilefu, W.Huang, and C.G.Atkeson, “3D Walking Based on Online Optimization,” in *Proceedings of IEEE-RAS International Conference on Humanoid Robots (Humanoids)*, 2013, pp. 21–27.

[8] R.Tedrake, S.Kuindersma, R.Deits, and K.Miura, “A closed-form solution for real-time ZMP gait generation and feedback stabilization,” in *Proceedings of IEEE-RAS International Conference on Humanoid Robots (Humanoids)*, 2015, pp. 936–940.

[9] K. Kaneko, M. Morisawa, S. Kajita, S. Nakaoka, T. Sakaguchi, R. Cisneros, and F. Kanehiro.

[10] T. Sugihara, “Solvability-unconcerned inverse kinematics based on levenberg-marquardt method with robust damping,” in *Proceedings of 9th IEEE-RAS International Conference on Humanoid Robots*, 2009, pp. 555–560.

[11] S.Kajita, O.Matsumoto, and M.Saigo, “Real-time 3d walking pattern generation for a biped robot with telescopic legs,” in *Proceedings of the IEEE International Conference on Robotics and Automation*, 2001, pp. 2299–2306.

[12] T.Sugihara, Y.Nakamura, and H.Inoue, “Realtime humanoid motion generation through zmp manipulation based on inverted pendulum control,” in *Proceedings of the IEEE International Conference on Robotics and Automation*, 2002, pp. 1404–1409.

[13] Y.Tassa, N.Mansard, and E.Todorov, “Control-Limited Differential Dynamic Programming,” in *Proceedings of IEEE International Conference on Robotics and Automation*, May 2014.

[14] J.Pratt, J.Carff, S.Drakunov, and A.Goswami, “Capture point: A step toward humanoid push recovery,” in *Proceedings of IEEE-RAS International Conference on Humanoid Robots (Humanoids2006)*, 2006, pp. 200–207.

[15] T. Takenaka, T. Matsumoto, and T. Yoshiike, “Real Time Motion Generation and Control for Biped Robot –1st Report: Walking Gait Pattern Generation–,” in *Proceedings of IROS*, 2009, pp. 1084–1091.

[16] At L. Hof, “The ‘extrapolated center of mass’ concept suggests a simple control of balance in walking,” *Human Movement Science*, vol. 27, pp. 112–125, 2008.

[17] S. Nakaoka, “Choreonoid: Extensible Virtual Robot Environment Built on an Integrated GUI Framework,” in *Proceedings of the 2012 IEEE/SICE International Symposium on System Integration (SII2012)*, December 2012, pp. 79–85.

[18] K.Nagasaka, M.Inaba, and H.Inoue, “Stabilization of dynamic walk on a humanoid using torso position compliance control,” in *Proceedings of 17th Annual Conference of the Robotics Society of Japan*, 1999, pp. 1193–1194, (in Japenese).

[19] E.R. Westervelt, J.W. Grizzle, and D.E. Koditschek, “Hybrid Zero Dynamics of Planar Biped Walers,” *IEEE Transactions on Automatic Control*, vol. 48, no. 1, pp. 42–56, January 2003.

[20] H-H. Zhao, W-L. Ma, M.B. Zeagler, and A.D. Ames, “Human-Inspired Multi-Contact Locomotion with AMBER2, booktitle=Proceedings of the ACM/IEEE International Conference on Cyber Physical Systems (ICCPS), pages=199-210, year=2014,.”

[21] J. Reher, E.A. Cousineau, A. Hereid, C.M. Hubicki, and A.D. Ames, “Realizing Dynamic and Efficient Bipedal Locomotion on the Humanoid Robot DURUS,” in *Proceedings of the 2016 IEEE International Conference on Robotics and Automation (ICRA)*, 2016, pp. 1794–1801.

[22] A. Hereid, E.A. Cousineau, C.M. Hubicki, and A.D. Ames, “3D Dynamic Walking with Underactuated Humanoid Robots: A Direct Collocation Framework for Optimizing Hybrid Zero Dynamics,” in *Proceedings of the 2016 IEEE International Conference on Robotics and Automation (ICRA)*, 2016, pp. 1447–1454.

[23] D. Verscheure, Bram Demeulenaereet, Jan Swevers, Joris De Schutter, and Moritz Diehl, “Time-optimal path tracking for robots: A convex optimization approach,” *IEEE Transactions on Automatic Control*, vol. 54, no. 10, pp. 2318–2327, 2009.

[24] Kris Hauser, “Fast interpolation and time-optimization on implicit contact submanifolds,” in *RSS 2013*, 2013.